

Evaluation of preCICE in ESM regridding benchmark

IDP project

Alex Hocks  

School of Computation, Information and Technology, Technical University of Munich

 alex.hocks@tum.de

April 1, 2021

Abstract — In the field of Earth System Models, meshes do not align or match usually, necessitating the use of couplers. We evaluate preCICE, a general coupling library, in this field by comparing it to commonly used and specialised couplers of this field. This is done by reproducing the benchmark by Valcke et al. [1]. The process of using preCICE is described and results are evaluated leading to the conclusion that in the current state the trade-off between conservational properties and target mesh accuracy needs to be considered.

1 Introduction

Be it in the field of Meteorology for the next weather forecast or other topics involving a representation of the whole Earth, Earth System Models (ESMs) are used for this purpose. These models often comprise different meshes representing their respective aspect, such as atmosphere (ATM) and ocean (SEA) meshes. Given non-monolithic solvers, simulations carried out on ESMs require different solvers for each mesh. To transfer effects from boundary regions of one mesh to another, the solvers require coupling. Towards this extend, there exist different coupling libraries that perform the mapping of values from one mesh to another. In the Regridding Benchmark by Valcke et al. [1] a selection of such libraries were evaluated on different pairs of ESM meshes. The couplers selected in the paper were specialized for the usage with ESM meshes. The aim of this project is to evaluate preCICE - a generic coupling library - in the benchmark and compare the results to the original. The goal is to determine what the main differences are and if specialized couplers are necessary for these problems.

1.1 Meshes

As Earth is not a perfect sphere, we use the WGS84 model, resulting in an ellipsoid. ATM models are likely to be a shell around said ellipsoid, whilst SEA models may only contain a subsection of it. The re-

sulting meshes are different discretization approaches of these models. As the purpose of the Regridding Benchmark is the evaluation of the mapping from one mesh to another, the considered meshes only contain the boundary area, i.e. the surface of the WGS84 ellipsoid.

ATM meshes span across the entire ellipsoid, since there exist no gaps in the atmosphere. SEA meshes on the contrary should only be valid in the regions of oceans. Therefore, certain areas are masked out. All meshes are discretized into cells of not necessarily uniform geometry and number of points. Meshes are provided in two forms: a) Each cell is defined via the location of its corner points b) Each cell is defined via its center point.

The SEA meshes are called `torc` and `nogt`, both comprising quadrilateral cells whilst `nogt` being of higher resolution. The ATM meshes are called `boggd`, `icoh`, `icos` and `sse7`. `boggd` and `sse7` are constructed mostly from quadrilaterals. `sse7` has certain regions in which cells contains up to 7 points. `icoh` and `icos` are constructed from hexa- and pentagons. `icoh` has a significantly higher resolution than `icos`.

Meshes are expressed in two forms. a) 2D geodesic using lat/lon coordinates b) 3D cartesian using x/y/z coordinates. The original meshes are provided in NC files. Those only contain a 2D geodesic representation. For our purposes we convert those into 3D cartesian represenation.

1.2 Test Functions

To provide test data for the mapping 4 different test functions are evaluated on the meshes. These are:

- Sinusoid: Slowly varying standard sinusoid over the globe
- Harmonic: More rapidly varying function with 16 maximums and 16 minimums in northern and southern bands

- Vortex: Slowly varying function with two added vortices, one in the Atlantic and one over Indonesia
- Gulfstream: Slowly varying standard sinusoid with a mimicked Gulf Stream

The functions are evaluated using geodesic coordinates. See figure 1 for an example on the nogt mesh. The formal definition is provided in the reference paper [1].

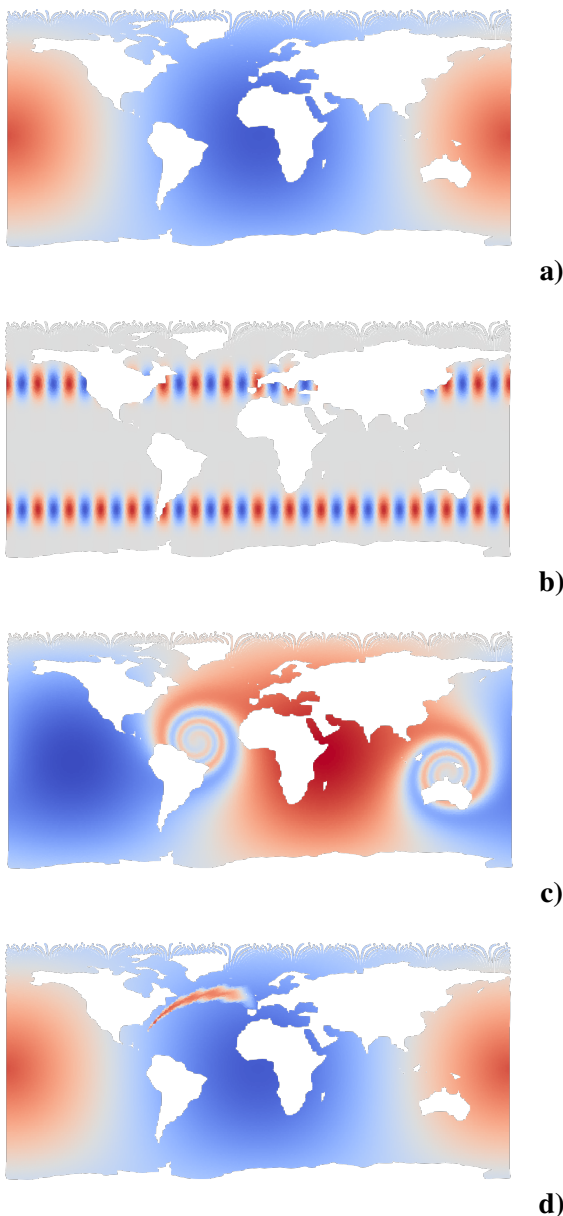


Figure 1 Mesh nogt evaluated on test functions. a) sinusoid
b) harmonic c) vortex d) gulfstream

1.3 Mapping Theory

Mapping values from one mesh to another is required, since mesh points usually do not align perfectly. Assuming we have a point \mathbf{x}_i^s on the source mesh, there usually is no point \mathbf{x}_j^t on the target mesh for which we can transfer the test function value $t(\mathbf{x}_i^s) =: y_i^s$ directly to \mathbf{x}_j^t as $\mathbf{x}_i^s \neq \mathbf{x}_j^t$.

Instead, we require a mapping $m_{\mathbf{x}_0^s, \mathbf{x}_1^s, \dots}(\mathbf{x}_j^t, y_0^s, y_1^s, \dots) = y_j^t$, that uses the source mesh points $\mathbf{x}_0^s, \mathbf{x}_1^s, \dots$ and source values y_0^s, y_1^s, \dots to determine the value at \mathbf{x}_j^t . We denote m only as a function of the source values and target point, since the source points are fixed for a given mesh.

1.4 Accuracy Metrics

We define Ψ^s, Ψ^t as the test function evaluated on the source and target mesh. $R\Psi^s$ is the test function on the source mesh mapped to the target mesh. I_s, I_t are integrals approximations on the source and target meshes, which are computed by the sum of cell areas multiplied by the function value. $M := |R\Psi^s - \Psi^t|/|\Psi^t|$ is the misfit.

As accuracy measures we consider the mean, max and rms of the misfit. Furthermore, we use $L_{\min} := (\min \Psi^t - \min R\Psi^s)/\max |\Psi^t|$ and $L_{\max} := (\max R\Psi^s - \max \Psi^t)/\max |\Psi^t|$. Source and target global conservation are $|I_t(R\Psi^s) - I_s(\Psi^s)|/I_s(\Psi^s)$ and $|I_t(R\Psi^s) - I_t(\Psi^t)|/I_t(\Psi^t)$.

1.5 Mappings in Paper

The mapping libraries used in the paper were SCRIP, YAC, ESMF and XIOS. When possible, the mappings were performed for all libraries using first and second order methods. Each had a conservative and non-conservative version.

2 Process with preCICE

Recreating the benchmark using preCICE required several preprocessing steps due to the format of the provided data. The entire process can split be into 6 steps. These are explained in the following subsections. All subsequent transformations from 2D geodesic to 3D cartesian and vice versa are performed using the Proj library bindings for Python. The used code, scripts and data can be found in our repository¹.

¹<https://github.com/Snapex2409/ESM-NC-VTK-Tool/tree/main>

2.1 SEA Masks

As only the SEA meshes have masks we need to transfer those to the ATM meshes in order to have a well posed mapping problem[1]. Towards this extend the representation for the masks is based on the meshes defined by the cells using their corner points. Therefore, we extract as the first step all the meshes from the NC files into VTK format. Each VTK file contains one mesh using a vtkUnstructuredGrids, in which each cell is given via its corner points in 3D cartesian coordinate system. For the SEA meshes we attach one vtkPointData array containing ones for all points, that are contained in sea-cells. This information is extracted from the masks NC file. It should be noted, that at this stage all duplicated points as well as points that differ only spuriously are merged into a single entity. Furthermore, connectivity information is added as it is required by the next step. This is done by performing a triangulation of the surface defined by the points of each cell. A triangulation was necessary since there exist meshes that contain cells with more than 4 points, whereas preCICE only supports geometries up to quads.

2.2 ATM Masks

To obtain valid masks for the ATM meshes, each SEA mesh mask is mapped to every ATM mesh using a conservative nearest-projection mapping with preCICE. The previously mentioned connectivity information is required due to the nearest-projection mapping. This results in two masks being created for every ATM mesh, one for each SEA mesh.

2.3 Mesh Extraction

The meshes used for the benchmarking purposes only use the center points of each cell. By using the original and mapped masks the sea content is evaluated for each cell through the average of the mask-values of its points. If the average is $< 1/1000$, then the cell is considered to be land and is removed[1].

As all meshed now only contain center points, no connectivity information between points exists explicitly. In order to reconstruct it, we consider which cells contained common points. Based on that potential edges are found. Afterwards only specific edges are selected, such that in the resulting mesh surface, there exist no triangles that overlap with each other. Furthermore, a vtkPointData array is attached

containing the areas of each cell. As a result we obtain two center based meshes for each ATM mesh, as there are two masks available. For the SEA meshes there is only a single output.

2.4 Function Evaluation

As the next step all test functions are evaluated on all meshes based on the center points. The evaluation results are attached as another vtkPointData array.

2.5 Mapping

We perform all possible mappings. When we map a SEA mesh a to an ATM mesh b , then we only use the ATM mesh that was created using the mask generated by a . The same applies for the opposite mapping direction as well. Mapping two SEA meshes requires no further precaution. When mapping ATM meshes with each other, we use the meshes created using the nogt mask since nogt has the highest resolution.

We perform all mappings using three different mapping methods supported by preCICE: nearest neighbour, nearest projection and radial basis function. As the radial basis function mapping requires further parameters, we fine tuned those for stable results. All mappings were performed using the 3D cartesian representation of the meshes.

2.6 Metrics Evaluation

As the final step we evaluate all mapping results based on the prior mentioned metrics. For this all mapping results need to be converted to 2D geodesic representation, because we need to compute analytical function evaluations on the target meshes. As output we create a file containing JSON with the mapping metrics as well as a further VTK file. The VTK file is based on the mapping result. However, we attach a further vtkPointData array containing the error metric, misfit, for each point.

3 Results of preCICE

We compare our results to the results from the original paper. For the papers non-conservative mappings we compare _DISTWGT_1 to nearest neighbour, _BILINEAR to nearest projection and _BICUBIC to radial basis function. For conservative mappings nearest neighbour is omitted and we compare _CONSERV_FRACAREA to nearest projection and

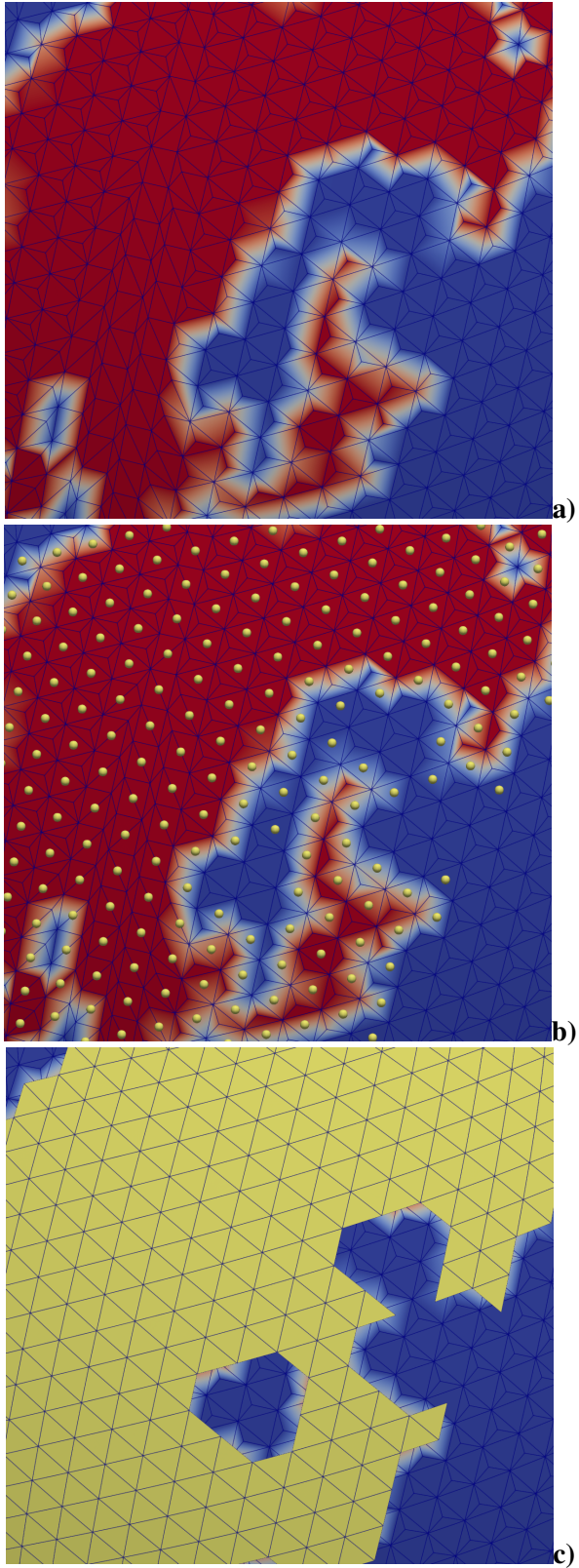


Figure 2 Mesh conversion process on icos. a) Corner based mesh containing mask information in each cell corner point
b) Overlayed center points for each valid cell using yellow points
c) Added connectivity information for center points

_CONS2ND_FRACAREA to radial basis function.

Comparing the non-conservative mapping, we observe that preCICE exhibits a similar behaviour in terms of misfit. In the majority of all cases, the misfit (mean, max or rms) is lower than the reference. This means that the error to the analytical solution on the target mesh is lower with preCICE. This coincides with the results displaying very small values for the target mesh conservation. On the other hand, when considering the source mesh conservation, preCICE is worse by approximately factor 3 to 10. See plots in figure 3. Furthermore, the source conservation for preCICE appears to be independent of mapping method and test function. This is also valid for the reference mappers, however to a smaller extent.

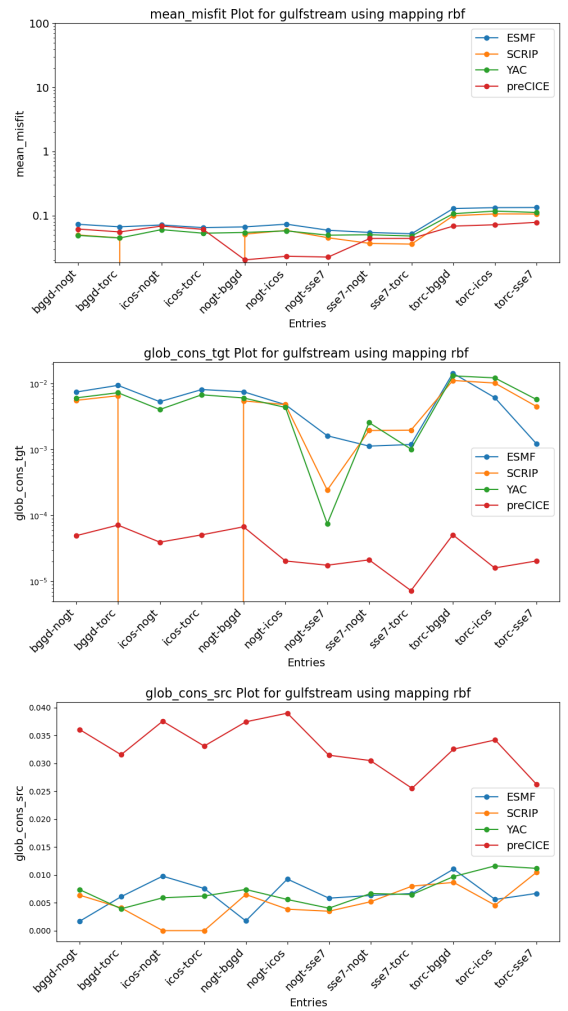


Figure 3 Overall representative behaviour of consistent pre-CICE mapping compared to non-conservative reference.

Considering max-misfits, then the results of preCICE follow the same trajectory as the refer-

ence's. For nearest-neighbour and nearest-projection mappings the max-misfits are almost identical. For radial basis function it is significantly less than the reference, with exception of the gulfstream cases. There rbf performs the same as the reference with respect to max-misfit. The only noteworthy difference overall is for the sinusoid test function with torc being the source mesh. This is highlighted in figure 4. The

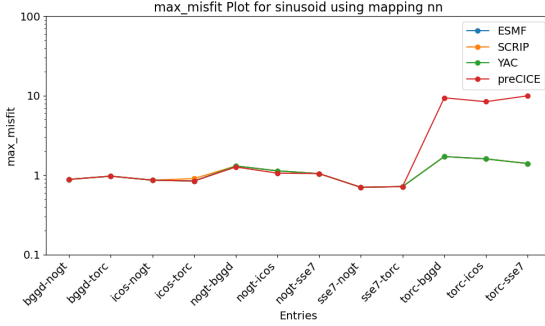


Figure 4 Maximum misfit of nearest neighbour mapping with malformed torc mesh for preCICE

higher maximum error can be located at a few cells around the south pole of the respective meshes. When analyzing those cells, one can identify that these cells should not exist, as they are part of Antarctica, thus, not part of the ocean. Upon checking the respective masks, it is apparent that the relevant cells were not masked out. Therefore, the issue lies within the mapping from the torc mesh mask to the target mesh. Since no mesh information exists in the torc mesh for a circular region A within the land region of the south pole, there are two small regions $r_{1,2}$ in the boundary of A in which the mask values are interpreted as ocean cells. When performing the mapping from the torc mesh mask to the target mesh, this results in cells being not masked out in the regions $r_{1,2}$ to the south pole, yielding the visible triangular areas, as displayed in figure 5. A similar issue arises in



Figure 5 Malformed torc mesh in antarctic region. Left: torc mesh mask Right: Error on bggd

region of the mediterranean ocean. Here, malformed

cells exist in the source (torc) mesh, connecting regions in north Africa to Saudi-Arabia. This results once more in necessary cell not being masked out, see figure 6. Therefore, the maximum misfit is higher. After removing these cells, the created masks are correct and the mapping results with preCICE display no significant deviation from the reference mappings. The behaviour of nearest-neighbour

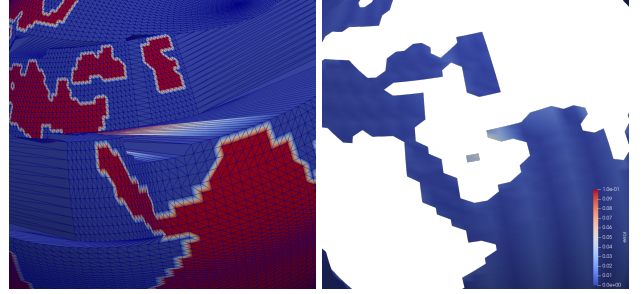


Figure 6 Malformed torc mesh in northern Africa. Left: torc mesh mask Right: Error on bggd

and nearest-projection being similar to the reference and rbf being better carry over to mean- and rms-misfit.

Regarding l-min and l-max, preCICE yields similar results as the reference without much deviation. For select cases l-min and l-max are closer to 0 with preCICE. This means that the mapping results over- or underestimate the target analytical function less, i.e., the target function is represented with higher accuracy. This is also reflected in the global target conservation. When viewing the target conservation with logarithmic y-axis scaling, we observe that preCICE is about 2 to 3 orders of magnitude smaller. An example is provided in figure 7.

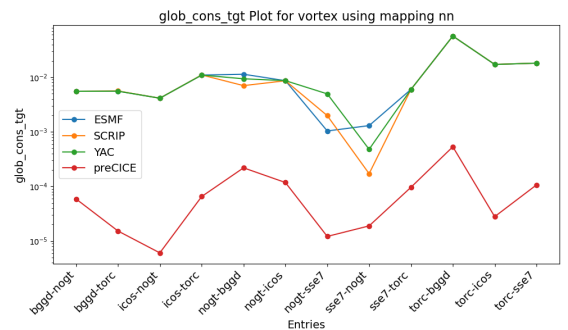


Figure 7 Global target conservation of consistent mappings using log scaling.

When performing a scaled-consistent mapping with preCICE, which is an approximation of the conservative mapping in the paper, the following observations are made. The mapped results have a higher error to

the analytical function on the target mesh. Thus, the target mesh conservation as well as misfits are across the board worse than in the consistent mapping. However, the source mesh conservation is now comparable to the results of the conservative and non-conservative mappings from the paper.

To determine the impact of the scaled-consistent mapping with preCICE we first compare the "conservative" results of preCICE with the consistent result of the reference. Checking the maximum misfits one can say, that our results are roughly in accordance with the reference. However, exceptions apply. In the nearest-neighbour and nearest-projection mappings for the sinusoid cases the max-misfit is higher by approximately factor 3. This behaviour extends to mean- and rms-misfits in which all mappings have higher misfit values for all cases, see figure 8. The l-min metric displays

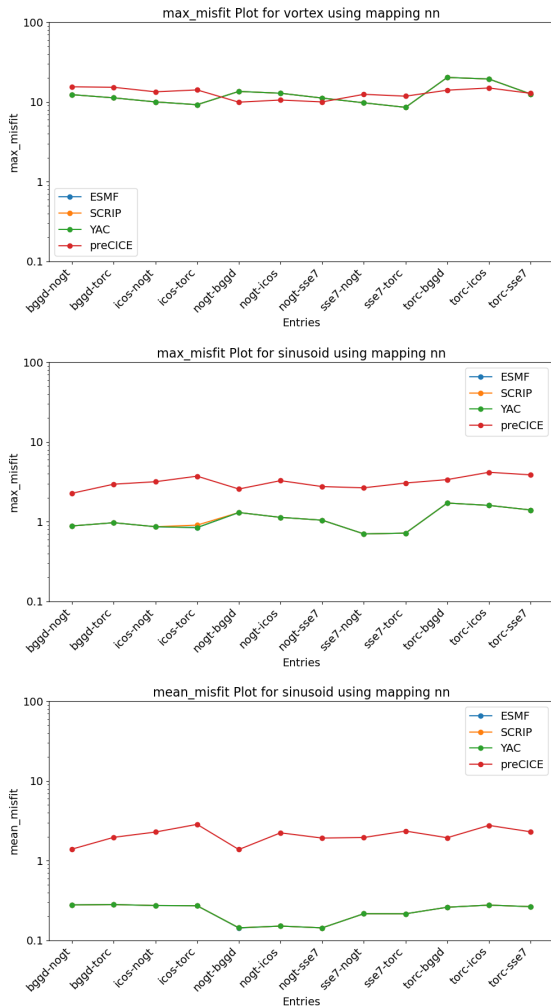


Figure 8 Misfits for scaled-consistent mapping in preCICE and non-conservative reference.

absolute values up to ≈ 0.04 while the reference is in most cases by multiple orders of magnitude closer to 0.

Only for the nearest-neighbour and nearest-projection mappings with the harmonic test function we observe that the reference deviates from 0 and that the preCICE results follow those. For all other cases there is a pattern visible independent of mapping and test function. A strongly correlated pattern can be found in the l-max results for preCICE, see figure 9. Whenever, l-min is less than 0 then l-max is greater than 0 and vice versa. This can be interpreted as the effects of the

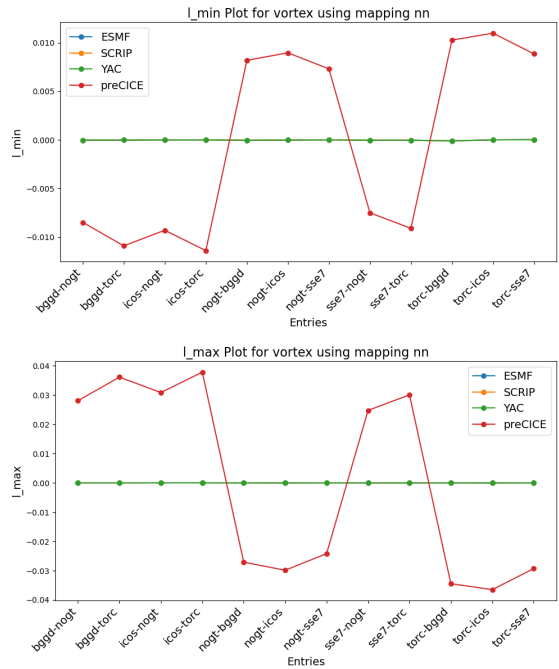


Figure 9 l-min and l-max correlation for scaled-consistent preCICE mapping with non-conservative reference.

scaled-consistent mapping. To verify this claim, we analyze the results in further detail. We observe pairs (-l-min, +l-max) and (+l-min, -l-max). Following the definition of these metrics:

- -l-min: minimum is larger
- +l-max: maximum is larger
- +l-min: minimum is smaller
- -l-max: maximum is smaller

Based on this we infer, that for (-l-min, +l-max) all values were scaled up by a factor $s > 1$ and for (+l-min, -l-max) scaled down by a factor $0 < s < 1$. When checking the minimum and maximum values of the respective meshes, this holds. This scaling occurs due to the nature of the scaled-consistent mapping in preCICE, in which first a consistent mapping is performed. Afterwards, the results are rescaled in a post-processing step to yield a conservative mapping. It can be defined as follows:

$$v_{tgt} = D M v_{src}$$

with v_{src} being the point data of each node and M the consistent mapping matrix. D is the rescaling matrix and can be obtained with:

$$D = s \cdot Id$$

s is the aforementioned scaling factor and is defined as the balancing factor to equate the surface integrals on the source and target mesh:

$$s = \frac{I_s(\Psi^s)}{I_t(R_{\text{cons}}\Psi^s)}$$

MASK	torc	nogt
icos	4.096	4.016
bggd	4.090	4.001
sse7	4.061	3.983
torc	3.941	—
nogt	—	3.844

Table 1 Filtered center mesh areas. All values are scaled by 10^{14}

Mapping	src area	tgt area	src/tgt	s_{real}
bggd-nogt	4.001	3.844	1.041	> 1
bggd-torc	4.090	3.941	1.038	> 1
icos-nogt	4.016	3.844	1.045	> 1
icos-torc	4.096	3.941	1.039	> 1
nogt-bggd	3.844	4.001	0.961	< 1
nogt-icos	3.844	4.016	0.957	< 1
nogt-sse7	3.844	3.983	0.965	< 1
sse7-nogt	3.983	3.844	1.036	> 1
sse7-torc	4.061	3.941	1.030	> 1
torc-bggd	3.941	4.090	0.964	< 1
torc-icos	3.941	4.096	0.962	< 1
torc-sse7	3.941	4.061	0.970	< 1

Table 2 Overview of mapping pairs with their respective mesh areas and their quotient, being an approximation for the scaling factor s . The resulting fractions are compared to the observed scaling scaling factors s_{real}

The previous assumptions regarding scaling are also supported by data, see the tables about mesh areas and area fractions. The first table contains the surface areas of all relevant meshes. When applying this information to all considered mapping pairs one can see that whenever the fraction of source mesh area to target mesh area is greater than one, so is the inferred scaling factor based on the l-min/l-max relation.

Using the information from table 2 we can assume that the scaling will change the data by up to approximately ± 4 percent-points. When checking the change from the consistent to scaled-consistent mapping results of mean-misfits, then we can see that the data lies within this threshold, figure 10. A similar effect can be seen

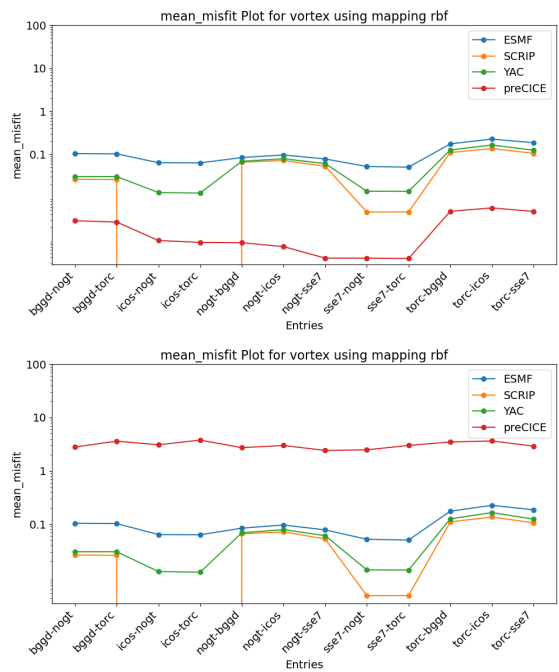


Figure 10 Mean misfit change from consistent to scaled-consistent mapping. Scaled-consistent mapping within 4 percent-points of error. Top: consistent Bottom: scaled-consistent

in the global target conservation, see figure 11. The deviation indicated here is also within the bounds of 4%. On the other hand, we observe a proportional reduction in the global source conservation. Hereby the results of preCICE are comparable to the reference.

As the final step, we compare the results of the scaled-consistent mapping with the conservative mappings of the reference. In terms of the misfit and l-min/max metrics, no significant changes are visible relative to the comparison conducted with the non-conservative reference mappings. The mean-misfits of preCICE remain at a higher level and l-min/max display the same correlation. The only noticeable change is in the source conservation metric. Here, the reference results are now lower, such that preCICE is overall worse by approximately factor 2 to 4, see figure 12. This holds for all mapping types independently of test function.

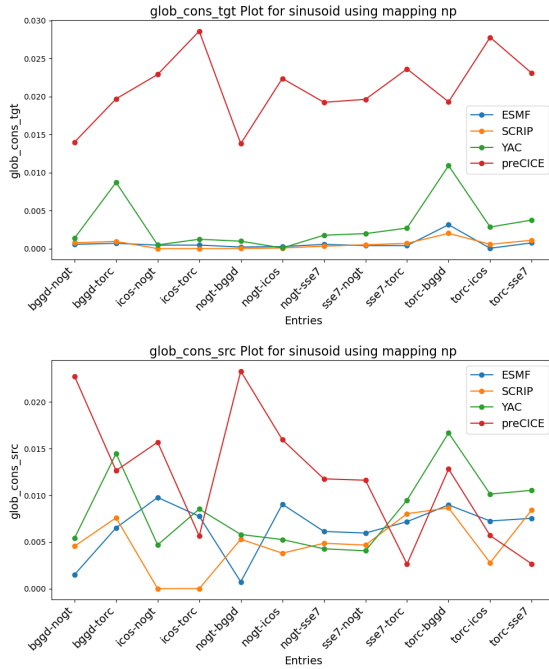


Figure 11 Global source and target conservation of scaled-consistent mapping.

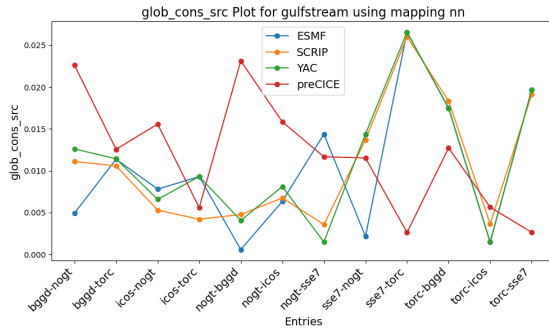


Figure 12 Global source conservation of scaled-consistent mapping with preCICE and conservative reference.

4 Conclusion

Using preCICE, a general coupling library, for ESM applications needs to be evaluated for each given use case. The issues we encountered with meshes and file formats in general, will most likely not arise when utilizing preCICE as a coupler in a real scenario between different solvers. For our reproduction of the benchmark, we did not use real solvers, only effectively mock-ups, to run the mappings. As those only accept VTK files, it required the conversion of data into this format. However, when using actual solvers, then meshes already exist for those, thus eliminating the issue.

The main benefit of applying preCICE is its ease of use and integration into other known solvers. However, re-

garding accuracy one must consider the trade-off we discussed between source and target conservation. If source conservation is not relevant, then preCICE is able to provide higher accuracy with its rbf mapping. On the other hand, if source conservation is of concern, then one must determine the overall disparity between surface areas of relevant meshes to obtain a rough estimate of the induced error by the scaled-consistent mapping. Based on that value, one can decide if preCICE is applicable for the use-case.

5 Outlook

In this work we only discussed the process of including preCICE in a ESM related mapping problem and evaluated it with respect to different accuracy metrics. As further steps, a detailed performance analysis in terms of runtime should be performed. Since preCICE is highly optimized for heavily parallel operations, it may be of value to evaluate different scenarios on distributed systems.

6 Reproducability Note

For detailed instructions see the documentation in our repository. All data is available in: <https://github.com/Snapex2409/ESM-NC-VTK-Tool/tree/main>. The initial readme file contains an overall overview, while the file reproducibility.md has more detailed instructions. All figures created by the benchmark are available in the images folder.

References

- [1] S. Valcke, A. Piacentini, and G. Jonville, “Benchmarking regridding libraries used in earth system modelling,” *Mathematical and Computational Applications*, vol. 27, no. 2, 2022. [Online]. Available: <https://www.mdpi.com/2297-8747/27/2/31>